Journal of Inorganic and General Chemistry
ZAAC
Zeitschrift für anorganische und allgemeine Chemie
DOI: 10.1002/zaac.202000030
ARTICLE

Structures and Stability of Complexes of $E(C_6F_5)_3$ (E = B, Al, Ga, In) with Acetonitrile

Nadezhda A. Shcherbina,[a] Anna V. Pomogaeva,[a] Anna S. Lisovenko,[a] Igor V. Kazakov,[a] Nikita Yu. Gugin,[a] Olesya V. Khoroshilova,[a] Yuri V. Kondrat'ev,[a] and Alexey Y. Timoshkin*[a]

Dedicated to Prof. Manfred Scheer on the Occasion of his 65th Birthday

Abstract. Complexes formed by interaction of $E(C_6F_5)_3$ (E = B, Al, Ga, In) with excess of acetonitrile (AN) were structurally characterized. Quantum chemical computations indicate that for $Al(C_6F_5)_3$ and $In(C_6F_5)_3$ the formation of a complex of 1:2 composition is more advantageous than for $B(C_6F_5)_3$ and $Ga(C_6F_5)_3$, in line with experimental observations. Formation of the solvate $[Al(C_6F_5)_3{\cdot}2AN]{\cdot}AN$ is in agreement with predicted thermodynamic instability of $[Al(C_6F_5)_3{\cdot}3AN]$. Tensimetry study of $B(C_6F_5)_3{\cdot}CH_3CN$ reveals its stability in the solid state up to 197 °C. With the temperature increase, the complex undergoes irreversible thermal decomposition with pentafluorobenzene formation.

Introduction

Donor-acceptor (DA) interactions between Lewis acids and Lewis bases[1] play important role in modern chemistry. The first donor-acceptor complex $BF_3{\cdot}NH_3$ was reported in 1809 by *Gay-Lussac*.[2] Lewis acids are widely used in catalysis, the Friedel–Crafts reaction,[3] was developed in 1877 long before the advent of the Lewis acid-base theory.[1] Despite of numerous examples of existing catalytic systems and continuous efforts to develop the new ones, catalysis with group 13 Lewis acids remains one of the most relevant and widely applicable both in laboratory practice and in industry. For example, $B(C_6F_5)_3$[4] is used as initiator for vinyl ether cationic polymerization in aqueous media,[5] and as a co-catalyst in the Ziegler–Natta reaction.[6] In past decade, $B(C_6F_5)_3$ as a classic Lewis acid is utilized for the construction of the frustrated Lewis pairs (FLP) for the activation of small molecules.[7–12] Radical anions $[B(C_6F_5)_3]^{-\bullet}$ and $[Al(C_6F_5)_3]^{-\bullet}$ are able to mediate the chemical reduction of O_2,[13,14] Se, Te, S_8, R–X–X–R (X = O, S, Te),[7] N_2O.[15] $Al(C_6F_5)_3$[16] demonstrates decent catalytic activity in polymerization of substituted butyrolactones[17] and benzofuran[18] forming high molecular weight polymers with narrow molecular weight distribution. It was found that $Al(C_6F_5)_3$ is the better catalyst than $B(C_6F_5)_3$ for the polymerization of L-lactide and ε-caprolactone.[19] $Ga(C_6F_5)_3$[16] and $In(C_6F_5)_3$[16] are prospective systems for CO_2 reduction.[20]

It is obvious that the catalytic activity depends on the strength of the Lewis acid. The most common acidity scales are based on the results of quantum chemical computations, for example, the values of gas phase H^-, F^-, Cl^-, CH_3^- affinity.[21] Another promising method is the comparison of enthalpy of gas phase dissociation of complexes with a neutral reference donor molecule. Computational studies indicate that the $B(C_6F_5)_3$ is the weakest acid in the $E(C_6F_5)_3$ (E = B, Al, Ga) series with respect to complex formation with ammonia due to the high energy of rearrangement of $B(C_6F_5)_3$.[22] However, this approach has not been applied to study the thermodynamic parameters for heavier analogs $In(C_6F_5)_3$ and $Tl(C_6F_5)_3$.[16] In addition, ammonolysis prevents experimental studies of ammonia complexes at high temperatures.[23,24] It was shown, that complex of $B(C_6F_5)_3$ with strong donor pyridine is thermally stable with respect to dissociation up to 220 °C, when the irreversible thermal destruction with C_6F_5H evolution takes place.[25]

Therefore, in this work a significantly weaker donor acetonitrile (AN) is chosen as the reference Lewis base. Complex $B(C_6F_5)_3{\cdot}AN$ was obtained and structurally characterized.[26] However, its thermal behavior was not studied. Complex of $In(C_6F_5)_3$ with acetonitrile of 1:1 composition is known[27] but no structural data were reported. In the present work, complexes obtained by the interaction of $E(C_6F_5)_3$ (E = B, Al, Ga, In) with excess of acetonitrile are studied experimentally and computationally.

Results and Discussion

Structural Studies

Reactions of $B(C_6F_5)_3$ and $E(C_6F_5)_3{\cdot}Et_2O$ (E = Al, Ga, In) with excess acetonitrile lead to isolation of solid donor-acceptor complexes $B(C_6F_5)_3{\cdot}AN$ (**1**), $[Al(C_6F_5)_3{\cdot}2AN]{\cdot}AN$ (**2**),

* Prof. Dr. A. Y. Timoshkin
E-Mail: a.y.timoshkin@spbu.ru
[a] Department of Inorganic Chemistry
St. Petersburg State University
Universitetskaya emb. 7–9
St. Petersburg, 199034 Russia
Supporting information for this article is available on the WWW under **http://dx.doi.org/10.1002/zaac.202000030** or from the author.

$Ga(C_6F_5)_3$·AN (**3**), and $In(C_6F_5)_3$·2AN (**4**), which were characterized by X-ray structural analysis. It should be noted, that $B(C_6F_5)_3$ and $Ga(C_6F_5)_3$ form with acetonitrile complexes in ratio 1:1 (compounds **1** and **3**), while aluminum and indium central atoms in **2** and **4** coordinate two molecules of acetonitrile. In addition, **2** contains one external acetonitrile molecule which is not bound to the aluminum. The molecular structures of **1**–**4** are presented in Figure 1, crystal data and experimental details are summarized in Table 1. The obtained experimental data are in good agreement with the previously described structure of $B(C_6F_5)_3$·AN.[26] Compounds **1** and **3** are isostructural. The distortion of EC_3 moiety from planarity (sum of the C–E–C angles 360°) is insignificant for trigonal bipyramidal complexes **2** and **4** [359.9(2)° and 359.9(1)°], and noticeable for tetrahedral complexes of 1:1 composition **1** and **3** [342.3(2)° and 349.7(2)°].

Valence E–N–C angles deviate from the perfect 180° found by computational studies for C_3 symmetric gaseous complexes of 1:1 and 1:2 composition. Experimental values are 177.0(1), 167.5(2)–171.1(2), 173.6(2), and 171.9(1) for **1**, **2**, **3**, and **4** respectively.

Computation Study

Optimized structures of C_3 symmetric gaseous complexes of 1:1 and 1:2 compositions are close to experimental ones. It is known that bond lengths, computed by quantum-chemical methods for the gas phase complexes, are slightly overesti-

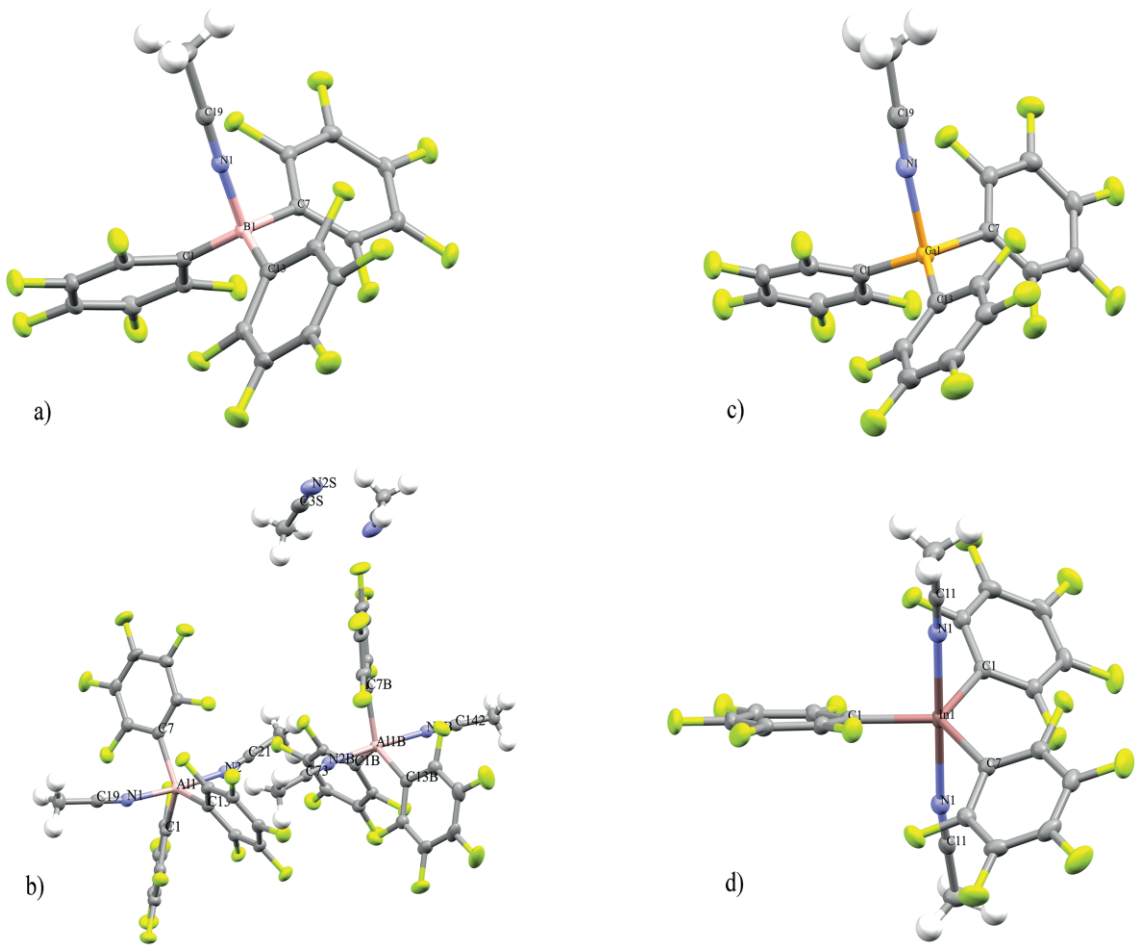

Figure 1. Molecular structures in the crystal: (a) **1**; (b) **2**; (c) **3**; (d) **4**. Ellipsoids are at 50% probability level. Selected bond lengths /Å and valence angles /°: for **1** B1–N1 1.6113(18), B1–C1 1.6356(19), B1–C7 1.633(2), B1–C13 1.637(2), N1–C19 1.1355(18), N1–B1–C1 105.61(10), N1–B1–C7 104.15(10), N1–B1–C13 103.18(10), C1–B1–C13 115.38(11), C7–B1–C13 115.33(11), C1–B1–C7 111.60(11); for **2** Al1–N1 2.082(2), Al1–N2 2.090(2), Al1–C1 2.008(2), Al1–C7 2.018(2), Al1–C13 2.016(2), N1–C19 1.138(4), N2–C21 1.138(4), N2S–C3S 1.133(4), Al1B–N1B 2.097(2), Al1B–N2B 2.083(2), Al1B–C1B 2.009(2), Al1B–C7B 2.004(2), Al1B–C13B 2.015(2), N1B–C142 1.142(4), N2B–C73 1.143(4), N1–Al1–N2 174.80(9), N1–Al1–C1 91.86(10), N1–Al1–C7 88.45(10), N1–Al1–C13 93.2(1), N2–Al1–C7 86.39(9), N2–Al1–C1 91.33(9), C1–Al1–C7 120.78(10), C1–Al1–C13 114.44(10), C7–Al1–C13 124.67(10), N1B–Al1B–N2B 175.48(9), N1B–Al1B–C1B 90.36(9), N1B–Al1B–C7B 90.03(10), N1B–Al1B–C13B 86.64(10), N2B–Al1B–C7B 92.33(10), N2B–Al1B–C1B 92.12(10), C1B–Al1B–C7B 115.36(10), C1B–Al1B–C13B 121.89(10), C7B–Al1B–C13B 122.65(10); for **3**: Ga1–N1 2.0467(19), Ga1–C1 1.981(2), Ga1–C7 1.985(2), Ga1–C13 1.981(2), N1–C19 1.122(3), N1–Ga1–C1 101.91(8), N1–Ga1–C7 100.61(8), N1–Ga1–C13 99.95(8), C1–Ga1–C7 112.19(9), C1–Ga1–C13 118.52(9), C7–Ga1–C13 118.97(9); for **4**: In1–N1 2.4557(15), In1–C1 2.1677(16), In1–C7 2.160(2), N1–C11 1.135(2), N1–In1–N1' 179.76(7), C1–In1–C7 119.46(4), C1–In1–N1 91.93(5), C1–In1–C1' 121.08(8), C1'–In1–N1 87.95(5), C7–In1–N1 90.12(3).

Table 1. Crystal data and structure determination parameters for **1**–**4**.

	1	**2**	**3**	**4**
Formula	$C_{20}H_3F_{15}BN$	$C_{24}H_9AlF_{15}N_3$	$C_{20}H_3F_{15}GaN$	$C_{22}H_6F_{15}InN_2$
M_w /g·mol^{-1}	553.04	651.32	611.95	698.11
Crystal system	monoclinic	orthorhombic	monoclinic	monoclinic
Space group	$P2_1/n$	$Pbc2_1$	$P2_1/n$	$C2/c$
a /Å	10.9467(3)	14.22192(14)	11.1268(3)	15.6505(3)
b /Å	9.22322(18)	21.53261(19)	9.4861(3)	11.929349(15)
c /Å	19.2484(4)	16.58381(18)	19.7677(6)	13.5931(3)
α /°	90	90	90	90
β /°	90.1140(19)	90	92.223(3)	111.461(2)
γ /°	90	90	90	90
V /Å^3	1943.39(7)	5078.54(9)	2084.91(11)	2361.88(7)
Z	4	8	4	4
No. reflections	33628	31074	17361	21979
No. indep. / R_{int}	3673 / 0.0448	9182 / 0.0311	4045 / 0.0515	2716 / 0.0294
No. param.	335	781	335	184
R_1 / wR_2 [$I \geq 2\sigma$ (I)]	0.0276 / 0.0706	0.0275 / 0.0712	0.0354 / 0.0942	0.0184 / 0.0480
GOF	1.033	1.039	1.047	1.089

Table 2. Selected characteristics for gaseous complexes. Donor-acceptor bond length R_{E-N} (Å, experimental data for the solid compounds in curly brackets), standard reaction enthalpies $\Delta_{diss}H°_{298}$ (kJ·mol^{-1}), standard reaction entropies $\Delta_{diss}S°_{298}$ (J·mol^{-1}·K^{-1}) for the process of gas-phase dissociation into the components, reorganization energies of the acceptor molecule upon complex formation $\Delta_{reorg}E$ (kJ·mol^{-1}), donor-acceptor bond energy (per bond) E_{DA} (kJ·mol^{-1}), the natural atomic charges on E q_E and N q_N, charge transfer values q_{CT} in ē, maximum of the electrostatic potential at the isodensity surface V_{max} (kcal·mol^{-1}), $E(2)$ (kcal·mol^{-1}) for $n(N)\rightarrow n^*(E)$ orbital interaction. M06–2X/def2-TZVP level of theory.

Compound	R_{E-N}	$\Delta_{diss}H°_{298}$	$\Delta_{diss}S°_{298}$	$\Delta_{reorg}E$(LA)	E_{DA}	q_E	q_N	q_{CT}	V_{max}	$E(2)$
$B(C_6F_5)_3$·AN	1.598, {1.611(2)}	69.8	121.4	87.2	164.2	0.391	–0.264	0.415	8.0	–
$Al(C_6F_5)_3$·AN	1.985	129.6	124.8	27.0	162.5	1.604	–0.461	0.176	31.7	117.6
$Ga(C_6F_5)_3$·AN	2.105, {2.047(2)}	99.3	94.9	21.1	125.9	1.516	–0.430	0.165	32.8	97.1
$In(C_6F_5)_3$·AN	2.342	90.5	96.9	11.1	106.9	1.563	–0.418	0.141	42.9	74.5
$Tl(C_6F_5)_3$·AN	2.557	62.4	109.2	3.3	70.9	1.394	–0.389	0.106	42.1	48.4
$B(C_6F_5)_3$·2AN	2.666, 2.656	50.4	221.2	1.8	31.2	0.980	–0.348	0.060		24.1,24.7
$Al(C_6F_5)_3$·2AN	2.120 {2.082(2), 2.090(2)}	184.2	253.8	10.0	102.3	1.550	–0.411	0.145		77.6
$Ga(C_6F_5)_3$·2AN	2.310, 2.312	140.3	231.5	5.6	78.0	1.499	–0.383	0.124		60.5,60.7
$In(C_6F_5)_3$·2AN	2.480, {2.4557(15)}	143.3	209.6	4.7	78.9	1.515	–0.383	0.117		55.1
$Tl(C_6F_5)_3$·2AN	2.687, 2.688	103.9	182.2	1.8	57.8	1.360	–0.367	0.087		38.7

mated compared to the experimental bond lengths for the solid compounds. This holds true for donor-acceptor bond lengths in complexes **2**–**4** where the difference between computed and experimental bond lengths are 0.038(2), 0.058(2), and 0.024(2) Å for **2**, **3** and **4**, respectively. However, for the B–N bond length in **1** the situation is different. Gas phase value of 1.598 Å computed at M06–2X/def2-TZVP level of theory is by 0.013(2) Å *shorter* than the experimental value for the solid complex.

Selected structural and thermodynamic parameters for studied complexes are summarized in Table 2. For 1:1 complexes standard dissociation enthalpy $\Delta_{diss}H°_{298}$ is the smallest for $B(C_6F_5)_3$·AN, which is associated with a significant reorganization energy of the Lewis acid $B(C_6F_5)_3$ (87 kJ·mol^{-1}). Note that reorganization energies decrease in order B >> Al > Ga > In > Tl. For complexes of 1:2 composition, reorganization energies are much smaller and do not exceed 10 kJ·mol^{-1}, since the acceptor moiety retains planar arrangement.

Computations show, that pyramidalization of the acceptor moiety upon complexation with formation of 1:1 complexes decreases LUMO energy of $E(C_6F_5)_3$ by 0.34, 0.43, 0.34, 0.26, 0.10 eV for E = B, Al, Ga, In, Tl, respectively; facilitating the orbital interaction. The highest decrease is observed for $Al(C_6F_5)_3$, which forms more thermodynamically stable complex. In complexes of 1:2 composition the LUMO energy of $E(C_6F_5)_3$ decreases by less than 0.09 eV.

For the complex $B(C_6F_5)_3$·2AN the optimized B–N distances are by 1.09 Å larger than the sum of covalent radii (1.58 Å[28]) but less than the sum of van der Waals radii of B and N (3.62 Å[28]). In consequence, the dissociation energy of such complex is small and the energy of the DA bond is only 31 kJ·mol^{-1}, the weakest among all studied complexes of 1:2 composition. In contrast, for complexes of 1:1 composition the DA bond energies decrease in order B ≥ Al > Ga > In > Tl (Table 2). As a result, complex $B(C_6F_5)_3$·2AN is thermodynamically unstable with respect to dissociation into $B(C_6F_5)_3$·AN and acetonitrile. The standard enthalpies of dissociation of complexes 1:2 into 1:1 and AN are –19, 55, 41, 53, and 42 kJ·mol^{-1} for B, Al, Ga, In, and Tl, respectively. The dissociation energies of complexes $Ga(C_6F_5)_3$·2AN and $Tl(C_6F_5)_3$·2AN are by 10 kJ·mol^{-1} smaller than those for their aluminum and indium analogs. The much smaller affinity of

boron in $B(C_6F_5)_3$·AN towards the second Lewis base can be rationalized on the analysis of distribution of the molecular electrostatic potential (MEP).[29] Maximum of the electrostatic potential at the isodensity surface V_{max} increases in order B < Al ≤ Ga < In ≤ Tl (Table 2). In case of complex $Al(C_6F_5)_3$·AN, there is a positively charged region on Al center (Figure 2d) which is absent on the boron analog $B(C_6F_5)_3$·AN (Figure 2c). It is also clear that upon complex formation the electrostatic potential on F atoms of C_6F_5 groups greatly increases, suggesting that the transferred charge is located on fluorine atoms of C_6F_5 groups. The orbital energy diagrams and shapes of LUMO orbitals for B and Al complexes are provided in the Supporting Information.

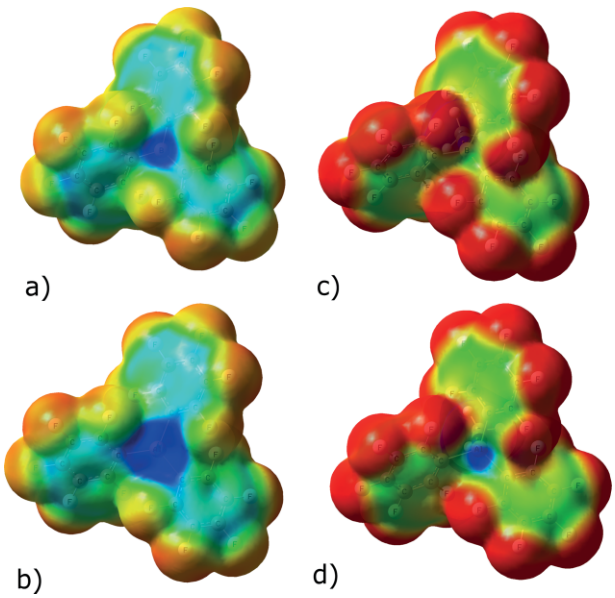

Figure 2. MEP on the isodensity surface with ρ = 0.001 for (a) $B(C_6F_5)_3$; (b) $Al(C_6F_5)_3$; (c) $B(C_6F_5)_3$·AN; (d) $Al(C_6F_5)_3$·AN. In complexes, the AN moiety is hidden behind the $E(C_6F_5)$ group. Color range: from –9.4 (red) to +25.1 (blue) kcal·mol^{-1}.

The structure of **2** deserves special attention. From the excess of the acetonitrile solvate $[Al(C_6F_5)_3$·2AN]·AN was crystallized. It is known that group 13 metal halides can form complexes of not only 1:1 and 1:2, but also 1:3 composition.[30] However, in case of **2**, only solvate of 1:2 complex is present in the solid state. Therefore, additional computational studies of complex of 1:3 composition $[Al(C_6F_5)_3$·3AN]·(both meridional and facial isomers) have been performed. Optimized structures are presented in Figure 3. *mer* isomer is by 32 kJ·mol^{-1} more stable than *fac* isomer. The Al–N–C angles in the optimized structures are 161.5–176.4° for *mer* and 150.7–156.1° for *fac* isomers. Reorganization energies for *mer* and *fac* isomers are very large: 144 and 206 kJ·mol^{-1}, respectively. Note that this large distortion of *fac* isomer leads to lowering of LUMO by 1.95 eV (compared by 0.28 eV for *mer* isomer). Despite sizeable DA bond energies (*mer* 112, *fac* 122 kJ·mol^{-1} per bond), dissociation of 1:3 into 1:2 complex and free AN in the gas phase is highly exergonic (at room temperature $\Delta_{diss}G°_{298}$ is less than –50 kJ·mol^{-1}), in line with experimental observation of absence of 1:3 complex.

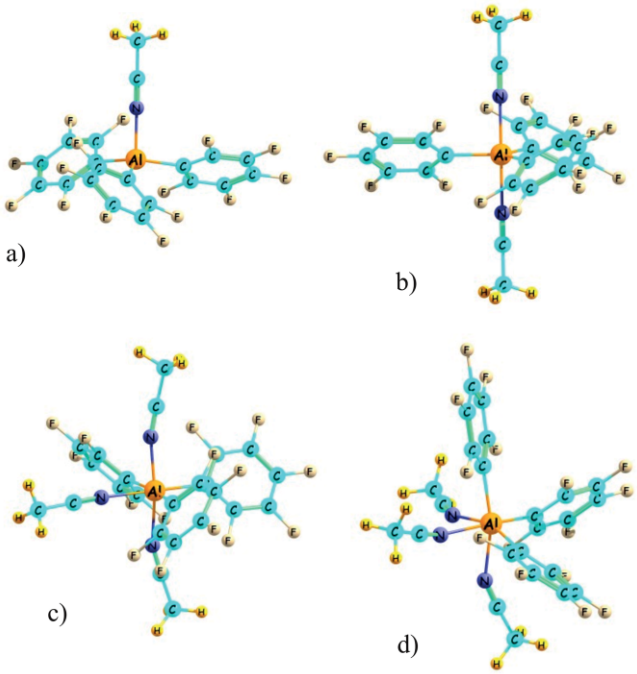

Figure 3. Optimized geometries of $Al(C_6F_5)_3$ complexes: (a) $Al(C_6F_5)_3$·AN; (b) $Al(C_6F_5)_3$·2AN; (c) *mer*-$Al(C_6F_5)_3$·3AN; (d) *fac*-$Al(C_6F_5)_3$·3AN.

Compared to free AN, the C≡N stretching mode is blue-shifted upon complex formation by 9–83 cm^{-1} in line with experimental observations for BF_3 complexes.[31]

This shift does not correlate with dissociation enthalpy of the complex.[29] However, for gaseous 1:1 and 1:2 complexes, the square root of C≡N stretching frequency shift Δν correlates with the energy of the DA bond (Figure 4) [Equation (1)]:

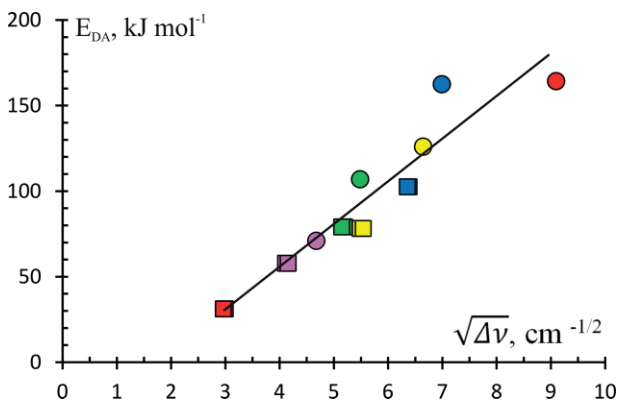

Figure 4. Correlation between the energy of DA bond and C≡N stretching mode frequency shift for gaseous $E(C_6F_5)_3$·*x*AN complexes [*x* = 1 circles, *x* = 2 squares; E = B (red), E = Al (blue), E = Ga (yellow), E = In (green), E = Tl (magenta)].

$$E_{DA} = (23.9 \pm 2.2)\sqrt{\Delta\nu} - (41 \pm 13);\ R^2 = 0.90 \quad (1)$$

In both polar and non-polar solvents, dissociation energy of $B(C_6F_5)_3$·AN and $Al(C_6F_5)_3$·AN complexes increases by about 10 kJ·mol^{-1} (Table 3). Situation is different for complexes $Ga(C_6F_5)_3$·AN and $In(C_6F_5)_3$·AN, where dissociation energy in

Table 3. Thermodynamic characteristics (dissociation energies $\Delta_{diss}E$, standard enthalpies $\Delta_{diss}H°_{298}$ and standard Gibbs energies $\Delta_{diss}G°_{298}$, all in kJ·mol^{-1}) of the dissociation reaction of $E(C_6F_5)_3$·AN complexes into components in the gas phase and in solvents. M06–2X/6-311++G** level of theory.

Compound	Gas phase			Acetonitrile			Benzene		
	$\Delta_{diss}E$	$\Delta_{diss}H°_{298}$	$\Delta_{diss}G°_{298}$	$\Delta_{diss}E$	$\Delta_{diss}H°_{298}$	$\Delta_{diss}G°_{298}$	$\Delta_{diss}E$	$\Delta_{diss}H°_{298}$	$\Delta_{diss}G°_{298}$
$B(C_6F_5)_3$·AN	78	72	29	89	83	37	88	82	34
$Al(C_6F_5)_3$·AN	136	131	92	146	141	112	147	141	99
$Ga(C_6F_5)_3$·AN	104	99	68	87	83	57	104	99	58
$In(C_6F_5)_3$·AN	97	92	58	65	60	26	89	87	52

the solvent decreases. At M06–2X/6-311++G** level of theory, $Ga(C_6F_5)_3$ and $In(C_6F_5)$ are stabilized by the solvent to a much greater extent than their complexes, in which the polarizability of the central atom is shielded by the bound acetonitrile. Energetic values in benzene solution and in the gas phase are close, indicating that benzene solution is a good approximation to the gas phase.

For the characterization of stability and volatility of complexes, mass-spectrometry, tensimetry and calorimetry studies were performed.

Mass-Spectrometry Study

Heating of **1** in vacuo results in full dissociation of the complex at 370 K [only $B(C_6F_5)_3^+$, CH_3CN^+ and their fragmentation products were observed in MS]. In case of **2** ion CH_3CN^+ is observed at 320 K, which is attributed to the loss of the excess acetonitrile. At 450 K ion $Al(C_6F_5)_3CH_3CN^+$ is appeared, that can be assigned to vaporization of complex of 1:1 composition $Al(C_6F_5)_3$·AN. For **3**, ions $Ga(C_6F_5)_3CH_3CN^+$, $Ga(C_6F_5)_3^+$, $Ga(C_6F_5)_2^+$, CH_3CN^+ are detected at 450 K, which indicates presence of $Ga(C_6F_5)_3$·AN complex in vapors. In case of **4** ion CH_3CN^+ is observed above 340 K, which is attributed to the loss of the excess acetonitrile. At 445 K ions $In(C_6F_5)_3CH_3CN^+$, $In(C_6F_5)_3^+$, $In(C_6F_5)_2^+$, CH_3CN^+ are observed, which can be attributed to vaporization of complex of 1:1 composition $In(C_6F_5)_3$·AN.

Note however, that at higher temperatures ion $C_6F_5H^+$ was detected in the mass-spectra (at 360 K, 320 K, 450 K, and 330 K for complexes **1**, **2**, **3**, and **4**, respectively). This indicates that irreversible thermal destruction with formation of pentafluorobenzene is competitive with loss of AN and vaporization of the complexes. In case of **2**, irreversible thermal destruction process is dominant in the temperature range 340–500 K ($C_6F_5H^+$ is the most intensive ion in the mass-spectrum). Ion $C_6F_5H^+$ was previously reported at 398 K in mass-spectra (EI, 20 eV) of $In(C_6F_5)_3$ complexes with AN, Et_2O, DMAP,[27] in agreement with data obtained in present report.[29]

Heating **2** and **4** result in loss of excess acetonitrile in temperature range 320–420 K with formation of more stable $Al(C_6F_5)_3$·AN and $In(C_6F_5)_3$·AN. Intensities of ions $E(C_6F_5)_3$·AN$^+$ in mass-spectra above **2–4** are low, which can be explained by dissociation of the complexes. Temperatures of appearance of $E(C_6F_5)_3^+$ ions in MS increase in order B (370 K) < In (445 K) ≤ Al(450 K) ≈ Ga (450 K).

Tensimetry Study of 1

The tensimetry study of **1** reveals formation of the solid complex $B(C_6F_5)_3$·$AN_{0.95\pm0.05}$, which is within the experimental errors agrees with expected complex of 1:1 composition. In excess of AN, solid $B(C_6F_5)_3$·AN is stable with respect to dissociation up to 470 K. Above 470 K, the complex undergoes irreversible thermal decomposition with pentafluorobenzene formation.[29]

Calorimetry Study

Brutto heat effects of the processes, which compounds **1** and **3** undergo under vacuum (residual pressure circa 0.09 Torr) at 358 K (for **1** and **3**) and 434 K (for **1**), were measured by a drop-calorimetry method.[32] It was found that **1** undergoes very slow (circa 57 h) endothermic process at 358 K and reduced (ca. 0.09 Torr) pressure, followed by slow exothermic thermal decomposition. At 434 K, endothermic process finishes after 0.5 h and slow exothermic thermal decomposition follows. Additional experiments on characterization of volatile reaction products of thermal decomposition of **1** revealed formation of pentafluorobenzene.[29] In the each experiment, white crystalline material was observed in the cold part of the apparatus and it is identical to the complex **1**. Since MS studies (vide supra) indicate the absence of $B(C_6F_5)_3$·AN complex in the gas phase, the endothermic process was ascribed to the heterogeneous dissociation [Equation (2)]:

$$B(C_6F_5)_3\cdot AN(s) \rightleftarrows B(C_6F_5)_3(g) + AN(g) \quad (2)$$

Estimated values for $\Delta_{(1)}H°$ are 221 ± 7 and 178 ± 9 kJ·mol^{-1} at 358 and 434 K, respectively.

In contrast, drop-calorimetric curve for **3** at 358 K exhibits sharp endothermic peak due to initial heating of the ampoule and **3**, followed by continuous exothermic peak (circa 40 h) attributed to irreversible thermal decomposition of **3** with ligand destruction. After the experiment, no sublimate was found in the cold part of the apparatus, non-volatile bulk remained in the measurement cell. The estimated brutto enthalpy for the thermal decomposition process of **3** at 358 K is –41 ± 11 kJ·mol^{-1}.[29]

Conclusions

Structures of tree new complexes $[Al(C_6F_5)_3$·2AN]·AN (**2**), $Ga(C_6F_5)_3$·AN (**3**), and $In(C_6F_5)_3$·2AN (**4**) were determined by

X-ray structural analysis. In excess of AN, only Al and In form solid complexes of 1:2 composition, while B and Ga form only 1:1 complexes. Computational studies reveal that dissociation enthalpies of 1:2 complexes into 1:1 complex and AN change nonmonotonically,[29] which may reflect the secondary periodicity.[33–35] Formation of 1:2 complexes in case of boron is thermodynamically unfavorable. Its heavier analogs can achieve higher coordination numbers, but with excess of AN, complexes of 1:2 composition are realized only for Al and In. Computational studies predict that complexes of 1:3 composition are unstable with respect to AN loss, which is in agreement with the observed structure of **2** in the solid state.

Mass-spectrometry study reveals absence of complex $B(C_6F_5)_3$·AN in vapors. Calorimetry study indicates that solid $B(C_6F_5)_3$·AN at 358 K and reduced pressure (< 0.1 Torr) undergoes slow heterogeneous dissociation into gaseous components (estimated dissociation enthalpy 221 ± 7 kJ·mol^{-1}). In excess of AN, solid $B(C_6F_5)_3$·AN is stable up to 470 K, where the irreversible thermal destruction with C_6F_5H evolution takes place.

In contrast to **1**, complexes $E(C_6F_5)_3$·AN (E = Al, Ga, In) are detected in vapors by MS method. All studied complexes irreversibly decompose with C_6F_5H evolution at elevated temperatures.

Experimental Section

Caution! Heating of complexes of $E(C_6F_5)_3$ (E = Al, Ga, In) with Et_2O and acetonitrile should be made with care, due to the risk of explosion.

General Procedures: All synthetic works were carried out using wholeglass systems under vacuum or in InertLab 2GB glove box in an argon atmosphere. Diethyl ether was dried using Na/benzophenone. Acetonitrile was dried with CaH_2. Deuterobenzene was dried with a mixture Na/K. All solvents were degassed by repetition of freezing-melting cycles under dynamic vacuum, stored over activated 4 Å zeolites and distilled under vacuum prior to use. Tris(pentafluorophenyl) borane $B(C_6F_5)_3$ (ABCR, 97 %) and aluminum trichloride (Sigma Aldrich, 99.99 %) were purified by sublimation in vacuo. Gallium and indium trichlorides were synthesized by the reaction of the respective metal (Ga 99.9999 %, in 99.99 %) with dry gaseous chlorine[36] in wholeglass systems and purified by sublimation in vacuo. $E(C_6F_5)_3$·Et_2O (E = Al, Ga, In) were synthesized according to *Pohlmann* and *Brinckmann*.[16]

NMR spectroscopy studies were performed on a Bruker AVANCE 400 instrument at room temperature. TMS and $CFCl_3$ were used as external standards. The resonance frequency in ^{1}H NMR is 400 MHz, ^{13}C{H} NMR is 100.6 MHz, ^{19}F{H} NMR is 376.5 MHz. Chemical shifts are given in ppm. IR spectroscopy measurements were performed on a Shimadzu IR Prestige-21 instrument. KBr pellets with samples were prepared under argon atmosphere in a glove box. X-ray phase analysis was performed on a Bruker D2 Phaser instrument with a copper anode. Mass spectral studies were performed on Thermoscientific ISQ quadruple mass-spectrometer with Direct Insertion Probe (DIP) equipment (electron ionization, 70 eV, m/Z range 15–1100 amu, measurement rate 5 spectra per second). Pressure in the ionization chamber is 10^{-5}–10^{-6} Torr. A sample (0.5–1 mg) was placed in thin glass ampoule (length 10 mm, diameter 1 mm) inside the glove box under argon. Ampoules were opened on air and immediately placed in DIP. Sample was heated from 50 °C to 300 °C with 10 K·min^{-1} heating rate. Gaseous products from sample were directly injected into the ionization chamber.

Synthesis of $B(C_6F_5)_3$·AN (1): 1 was synthesized in an argon atmosphere by dissolving $B(C_6F_5)_3$ (60 ± 1 mg, 0.12 mmol) in acetonitrile (160 ± 1 mg, 3.90 mmol) at room temperature. After evaporation of acetonitrile, large colorless crystals of **1** formed with quantitative yield. **^{1}H NMR** (C_6D_6): δ = s 0.33 (CH_3CN). **^{13}C{H} NMR** (C_6D_6): δ = s –1.20 (CH_3), s 114.00 (CN), t 114.93 (*ipso*-C_6F_5, J = 18 Hz), dm 137.44 (m-C_6F_5, J = 247 Hz), dm 140.68 (p-C_6F_5, J = 255 Hz), dm 148.16 (o-C_6F_5, J = 245 Hz). **^{19}F{H} NMR** (C_6D_6): δ = ddd –163.03 (m-F, C_6F_5, J_1 = 24.0, J_2 = 21.1, J_3 = 9.2 Hz), t –155.16 (p-F, C_6F_5, J = 21.1 Hz), dd –134.50 (o-F, C_6F_5, J_1 = 24.7, J_2 = 10.0 Hz). **MS** (EI, 70 eV, 423 K): (*m/z*,%,ion) 100.0 % $C_6F_3^+$ (*m/z* 129), 76.2 % $C_{11}F_5^+$ (*m/z* 227), 69.6 % $C_{12}F_7^+$ (*m/z* 277), 66.5 % $C_6F_4^+$ (*m/z* 148), 50.5 % $B(C_6F_5)_3^+$ (*m/z* 512), 50.2 % $C_{12}F_6^+$ (*m/z* 258), 28.0 % CH_3CN^+ (*m/z* 41), 23.7 % $C_{12}F_8^+$ (*m/z* 296), 15.7 % CH_2CN^+ (*m/z* 40), 14.7 % $C_{18}F_{12}^+$ (*m/z* 444), 12.0 % $B(C_6F_5)_2F^+$ (*m/z* 364), 11.7 % $BC_{11}F_8^+$ (*m/z* 295), 2.4 % $C_6F_5^+$ (*m/z* 167), 2.6 % $C_6F_5H^+$ (*m/z* 168). **IR** (KBr): $\tilde{\nu}$ = m 349, w 393, w 451, w 485, m 578, m 599, s 620, vs. 684, s 740, s 774, s 792, m 855, vs. 971, vs. 982, w 1013, w 1047, vs. 1108, s 1286, s 1384, vs. 1468, vs. 1521, w 1601, s 1650, w 2055, w 2100, w 2229, ν(C≡N) m 2366, m 2853, s 2924, br. m 3452 cm^{-1}.

Synthesis of $[Al(C_6F_5)_3$·2AN]*AN (2): 2 was synthesized in an argon atmosphere by dissolving $Al(C_6F_5)_3$·Et_2O (18 ± 1 mg, 0.029 mmol) in acetonitrile (400 ± 1 mg, 9.76 mmol) at room temperature. Slow (circa 48h) evaporation of acetonitrile leads to the formation of a colorless crystalline material with nearly quantitative yield. According to ^{19}F{H} NMR spectra, obtained material contains about 1 % of C_6F_5H as an impurity. **^{1}H NMR** (C_6D_6): δ = s 0.46 (CH_3CN). ^{13}C{H} (C_6D_6): s –0.80 (CH_3), other signals were not detected due to low solubility. **^{19}F {H} NMR** (C_6D_6): δ = m –162.38 (m-F, C_6F_5H), m –161.21 (m-F, C_6F_5), t –154.11 (o-F, C_6F_5H, J = 20.8 Hz), t - 152.15 (p-F, C_6F_5, J = 19.6 Hz), dd –139.13 (o-F, C_6F_{5H}, J_1 = 22.2, J_2 = 8.2 Hz), dd –123.24 (o-F, C_6F_5, J_1 = 27.0, J_2 = 11.6 Hz). **MS** (EI, 70 eV, 463 K): 100.0 % $C_6F_5H^+$ (*m/z* 168), 92.3 % $AlF_2CH_3CN^+$ (*m/z* 106), 58.6 % $C_6F_4^+$ (*m/z* 148), 58.0 % $C_5F_2H^+$ (*m/z* 148), 25.4 % $AlF_2C_6F_5^+$ (*m/z* 232), 16.5 % $AlF_2C_6F_5CH_3CN^+$ (*m/z* 254), 10.3 % $C_6F_3^+$ (*m/z* 129), 10.3 % CH_3CN^+ (*m/z* 41), 6.7 % $C_{12}F_8^+$ (*m/z* 296), 5.5 % CH_2CN^+ (*m/z* 40), 2.7 % $C_{12}F_7^+$ (*m/z* 277), 2.3 % $C_{12}F_6^+$ (*m/z* 258), 2.6 % $C_{11}F_5^+$ (*m/z* 227), 2.3 % $C_6F_5^+$ (*m/z* 167), 1.0 % $C_{18}F_{12}^+$ (*m/z* 444), 0.2 % $Al(C_6F_5)_3^+$ (*m/z* 528), 0.2 % $Al(C_6F_5)_3CH_3CN^+$ (*m/z* 569), 0.1 % $Al(C_6F_5)_2^+$ (*m/z* 361), 0.1 % Al^+ (*m/z* 27). **IR** (KBr): $\tilde{\nu}$ = w 424, w 472, m 506, m 557, w 612, w 718, w 744, vs. 957, m 1015, vs. 1071, m 1179, m 1271, m 1361, w 1381, vs. 1457, vs. 1512, s 1533, sh 1618, s 1644, sh 1652, w 2218, w 2250, ν(C≡N) m 2311, ν(C≡N) m 2340, m 2372, m 2850, m 2919, br. m 3431 cm^{-1}.

Synthesis of $Ga(C_6F_5)_3$·AN (3): 3 was synthesized in an argon atmosphere by dissolving $Ga(C_6F_5)_3$·Et_2O (247 ± 1 mg, 0.377 mmol) in acetonitrile (793 ± 1 mg, 19.3 mmol) at room temperature. Fast interaction of the components was observed to form a clear solution. Slow (circa 48h) evaporation of acetonitrile leads to the formation of a colorless crystalline material with 99 % yield. **^{1}H NMR** (C_6D_6): δ = s 0.29 (CH_3CN). **^{13}C{H} NMR** (C_6D_6): δ = s –0.74 (CH_3), t 112.23 (*ipso*-C_6F_5, J = 43 Hz), s 118.02 (CN), dm 137.22 (m-C_6F_5, J = 248 Hz), dm 141.89 (p-C_6F_5, J = 249 Hz), dm 148.97 (o-C_6F_5, J = 232 Hz). **^{19}F{H} NMR** (C_6D_6): δ = m –160.75 (m-F, C_6F_5), t –151.75 (p-F, C_6F_5, J = 21.3 Hz), dd –124.55 (o-F, C_6F_5, J_1 = 28.9, J_2 = 11.6 Hz). **MS** (EI, 70 eV, 463 K): 100.0 % $C_6F_3^+$ (*m/z* 129), 84.6 % $GaC_6F_6^+$ (*m/z* 255), 75.0 % Ga^+ (*m/z* 27), 70.7 % $Ga(C_6F_5)_2^+$ (*m/z* 403), 47.0 % $C_6F_4^+$

(*m/z* 148), 41.2 % CH_3CN^+ (*m/z* 41), 26.1 % $C_{12}F_7^+$ (*m/z* 277), 25.9 % $C_{12}F_8^+$ (*m/z* 296), 21.8 % CH_2CN^+ (*m/z* 40), 17.8 % $Ga(C_6F_5)_3^+$ (*m/z* 570), 13.0 % $C_6F_5^+$ (*m/z* 167), 12.6 % $C_6F_5H^+$ (*m/z* 168), 8.6 % $C_{11}F_5^+$ (*m/z* 227), 7.8 % $C_{12}F_6^+$ (*m/z* 258), 0.1 % $Ga(C_6F_5)_3CH_3CN^+$ (*m/z* 611). **IR** (KBr): $\tilde{\nu}$ = m 366, w 403, w 454, w 492, w 582, m 611, w 721, w 774, m 807, vs. 960, w 1013, w 1026, vs. 1070, s 1273, s 1369, vs. 1467, vs. 1512, s 1643, w 2250, ν(C≡N) w 2304, ν(C≡N) m 2333, w 2854, w 2924, w 2942, br. m 3430 cm^{-1}.

Synthesis of $In(C_6F_5)_3$·2AN (4): 4 was synthesized in an argon atmosphere by dissolving $In(C_6F_5)_3$·Et_2O (827 ± 1 mg, 1.20 mmol) in acetonitrile (810 ± 1 mg, 19.8 mmol) at room temperature. After circa 30 min a clear solution was formed. Slow (circa 48h) evaporation of acetonitrile leads to the formation of a colorless crystalline material with quantitative yield. **^{1}H NMR** (C_6D_6): δ = s 0.51 (CH_3CN). **^{13}C{H} NMR** (C_6D_6): δ = s –0.61 (CH_3), s 116.49 (CN), t 117.23 (*ipso*-C_6F_5, *J* = 27 Hz), dm 137.17 (m-C_6F_5, *J* = 260 Hz), dm 141.59 (p-C_6F_5, *J* = 238 Hz), ddm 148.86 (o-C_6F_5, J_1 = 231, J_2 = 22 Hz). **^{19}F {H} NMR** (C_6D_6): δ = m –162.30 (m-F, C_6F_5), t –152.71 (p-F, C_6F_5, *J* = 20.8 Hz), dd –119.02 (o-F, C_6F_5, J_1 = 30.6, J_2 = 10.5 Hz). **MS** (EI, 70 eV, 453 K): 100.0 % In^+ (*m/z* 115), 61.8 % $In(C_6F_5)_2^+$ (*m/z* 449), 32.4 % $InC_6F_6^+$ (*m/z* 301), 10.4 % $C_6F_5H^+$ (*m/z* 168), 7.8 % $C_6F_4^+$ (*m/z* 148), 7.5 % $C_6F_5^+$ (*m/z* 167), 5.6 % $In(C_6F_5)_3^+$ (*m/z* 616), 1.6 % $C_6F_3^+$ (*m/z* 129), 1.0 % $C_{12}F_8^+$ (*m/z* 296), 0.5 % $C_{11}F_5^+$ (*m/z* 227), 0.5 % CH_3CN^+ (*m/z* 41), 0.04 % CH_2CN^+ (*m/z* 40), 0.002 % $In(C_6F_5)_3CH_3CN^+$ (*m/z* 657). **IR** (KBr): $\tilde{\nu}$ = w 354, w 466, w 486, w 557, w 604, w 718, w 784, vs. 957, s 1012, vs. 1074, s 1266, s 1359, vs. 1464, vs. 1508, w 1610, m 1638w 2218, w 2249, ν(C≡N) m 2292, ν(C≡N) m 2319, m 2361, m 2851, m 2920, m 2951, m 3447 cm^{-1}.

X-ray Structural Analysis: For single-crystal X-ray diffraction experiment, crystals of **1**–**4** were fixed on a micro mount and placed on an Agilent Technologies SuperNova using CuK_α monochromated radiation diffractometers at a temperature of 100 K. For **4**, an Agilent Technologies Excalibur Eos diffractometer with monochromated MoK_α radiation was used. The unit cell parameters were refined by least square techniques. The structure have been solved by the direct methods and refined using SHELXL-97 program[37] incorporated in the OLEX2 program package.[38] The hydrogen atoms were placed in calculated positions and were included in the refinement in the 'riding' model approximation, with Uiso(H) set to 1.5Ueq(C) and C–H 0.96 Å for the CH_3 groups. Empirical absorption correction was applied in CrysAlisPro[39] program complex using spherical harmonics, implemented in SCALE3 ABSPACK scaling algorithm.

Crystallographic data (excluding structure factors) for the structures in this paper have been deposited with the Cambridge Crystallographic Data Centre, CCDC, 12 Union Road, Cambridge CB21EZ, UK. Copies of the data can be obtained free of charge on quoting the depository numbers CCDC-1971131 (**3**), CCDC-1971132 (**4**), CCDC-1971133 (**2**), and CCDC-1971134 (**1**) (Fax: +44-1223-336-033; E-Mail: deposit@ccdc.cam.ac.uk, http://www.ccdc.cam.ac.uk).

Tensimetry Study was performed using the automated static tensimetric method with a membrane null-manometer.[40,41] Freshly sublimed $B(C_6F_5)_3$ (50.09 ± 0.01 mg) in a glove box under argon was placed into the glass compartment (1.98 ± 0.01 mL), compartment was evacuated, sealed under vacuum and placed inside the tensimeter apparatus. Acetonitrile (circa 23.35 ± 0.01 mg,) was distilled into the tensimetry apparatus with internal volume of 21.73 ± 0.01 mL while cooling part of the chamber with liquid nitrogen. After that tensimeter was fused out, and heated to 160 °C at a rate of 10 K·h^{-1}. The amount of introduced acetonitrile (0.301 ± 0.002 mmol) was refined from the first two heating-cooling runs for pure acetonitrile using ideal gas expansion in the unsaturated vapor region. After that, a compartment with $B(C_6F_5)_3$ was mechanically broken. The amount of gaseous acetonitrile decreased, evidencing the formation of the solid complex $B(C_6F_5)_3$·$AN_{0.95\pm0.05}$, which is within the experimental errors agrees with expected complex of 1:1 composition. Subsequent heating/cooling runs reveal that solid complex $B(C_6F_5)_3$·AN is stable with respect to dissociation up to 197 °C. At 197 °C, complex undergoes irreversible thermal decomposition. At the end of the experiment, viscous dark brown solid state was visually observed in the inner volume, which indicates pyrolysis of the complex. Volatile decomposition products were condensed into a glass valve while cooling with liquid nitrogen. The valve was soldered from the system; after defrosting, a small amount of liquid was observed at room temerature. A valve with a sample of volatile components was opened under argon in an InertLab 2GB glove box. The sample was analyzed by ^{1}H, ^{19}F {H} NMR in $CDCl_3$. Analysis of the gas phase reveals formation of pentafluorobenzene.[29]

Computational Study: All computations were carried out using Gaussian 16 program package.[42] Three computational approaches have been used: (i) hybrid three-parameter exchange functional of Becke[43] with the gradient corrected correlation functional of Lee, Yang, and Parr[44] (B3LYP) with split valence def2-SVP basis set;[45] (ii) M06–2X high-nonlocality functional with the double amount of nonlocal exchange (2X)[46] with def2-SVP basis set; (iii) M06–2X functional with all electron def2-TZVP basis set.[45] The geometries of the compounds have been fully optimized with subsequent vibrational analysis. All structures correspond to minima on the respective potential energy surfaces. M06–2X functional provides results which are in qualitative agreement with the experimental data on $B(C_6F_5)_3$·Py complex.[25] Basis set superposition error (BSSE) was estimated using counterpoise method.[47] At M06–2X/def2-TZVP level of theory BSSE does not exceed 2.6 and 4.5 kJ·mol^{-1} for complexes of 1:1 and 1:2 composition, respectively. Taking into account that the counterpoise method overestimates BSSE,[48] in the results and discussion we used values obtained at M06–2X/def2-TZVP level of theory, uncorrected for BSSE. Solvent effects were taken into account using solvation energies of the compounds $\Delta_{solv}E$ computed using the SMD method[49] using gas phase optimized geometries at B3LYP/def2-SVP, M06–2X/def2-SVP, M06–2X/def2-TZVP levels of theory and with geometry optimization in the gas phase and in the solvent at M06–2X/6-311++G**(def2-TZVP ECP basis on In) level of theory. Molecular Electrostatic Potentials (MEP) were computed at M06–2X/def2-TZVP level of theory. The electrostatic potential is mapped at the isodensity surface with ρ = 0.001 ē/$Bohr^3$. The measure of the charge donation due to the orbital interaction can be estimated by a second order perturbation energy within NBO method.[50] The NBO property denoted as E(2) permits one to apply qualitative concepts of valence theory to describe the noncovalent energy lowering. Computed vibrational harmonic C≡N frequencies were scaled using scaling factor 0.9344, obtained from fitting experimental C≡N frequencies of isotopically substituted acetonitrile.[29]

Supporting Information (see footnote on the first page of this article): Synthetic procedures, NMR and IR spectra, mass spectrometry, tensimetry and calorimetry data, optimized geometries of compounds, computed total energies, enthalpies and entropies, thermodynamic characteristics, BSSE values, solvation energies in acetonitrile and benzene, LUMO energies, C≡N vibrational frequencies.

Acknowledgements

This work was financially supported by the Russian Science Foundation (grant no. 18–13–00196). Use of equipment of Resource centers "Magnetic resonance methods research", "X-ray diffraction methods research", "Chemical Analysis and Materials Research Centre" and "Computing Center" of the Scientific park of St. Petersburg State University is gratefully acknowledged. N.A.S. is grateful to SPSU travel grant 39423892.

Keywords: Group 13 tris(pentafluorophenyl) Lewis acids; Acetonitrile; Structure; Thermal stability; DFT computations

References

[1] G. N. Lewis, *Valence and the Structure of Atoms and Molecules*, Chemical Catalog Company, Inc. New York, USA **1923**, p. 172.
[2] J. L. Gay-Lussac, J. L. Thenard, *Mem. Phys. Chim. Soc. d'Arcueil* **1809**, *2*, 210–211.
[3] C. Friedel, J. M. Crafts, *Compt. Rend.* **1877**, *84*, 1392–1450.
[4] A. G. Massey, A. J. Park, *J. Organomet. Chem.* **1964**, *2*, 245–250.
[5] J. Zhang, Y. Wu, K. Chen, M. Zhang, L. Gong, D. Yang, S. Li, W. Guo, *Polymers* **2019**, *11*, 500.
[6] K. Nomura, G. Nagai, I. Izawa, T. Mitsudome, M. Tamm, S. Yamazoe, *ACS Omega* **2019**, *20*, 18833–18845.
[7] L. L. Liu, L. L. Cao, Y. Shao, D. W. Stephan, *J. Am. Chem. Soc.* **2017**, *139*, 10062–10071.
[8] G. C. Welch, R. R. S. Juan, J. D. Masuda, S. W. Douglas, *Science* **2006**, *314*, 1124–1126.
[9] A. Berkefeld, W. E. Piers, M. Parvez, *J. Am. Chem. Soc.* **2010**, *132*, 10660–10661.
[10] C. M. Mömming, E. Otten, G. Kehr, R. Fröhlich, S. Grimme, S. W. Douglas, G. Erker, *Angew. Chem. Int. Ed.* **2009**, *48*, 6643–6646.
[11] C. K. Bennett, M. N. Bhagat, Y. Zhu, Y. Yu, A. Raghuraman, M. E. Belowich, S. T. Nguyen, J. M. Notestein, L. J. Broadbelt, *ACS Catal.* **2019**, *9*, 11589–11602.
[12] J. Chen, L. Falivene, L. Caporaso, L. Cavallo, E. Y.-X. Chen, *J. Am. Chem. Soc.* **2016**, *138*, 5321–5333.
[13] J. T. Henthorn, S. Lin, T. Agapie, *J. Am. Chem. Soc.* **2015**, *137*, 1458–1464.
[14] X. Tao, C. G. Daniliuc, O. Janka, R. Pottgen, R. Knitsch, M. R. Hansen, H. Eckert, M. Lübbesmeyer, A. Studer, G. Kehr, G. Erker, *Angew. Chem. Int. Ed.* **2017**, *56*, 16641–16644.
[15] Y. Liu, E. Solari, R. Scopelliti, F. T. Fadaei, K. Severin, *Chem. Eur. J.* **2018**, *24*, 18809–18815.
[16] J. L. W. Pohlmann, F. E. Brinckmann, *Z. Naturforsch. B* **1965**, *20*, 5–11.
[17] Y. Zhang, G. M. Miyake, M. G. John, L. Falivene, L. Caporaso, L. Cavallo, E. Y.-X. Chen, *Dalton Trans.* **2012**, *41*, 9119–9134.
[18] F. Lin, M. Wang, D. Cui, *Macromolecules* **2017**, *50*, 8449–8455.
[19] Y. Nakayama, S. Kosaka, K. Yamaguchi, G. Yamazaki, R. Tanaka, T. Shiono, *J. Polym. Sci. Part A: Polym. Chem.* **2017**, *55*, 297–303.
[20] M. Xu, J. Possart, A. E. Waked, J. Roy, W. Uhl, D. W. Stephan, *Phil. Trans. R. Soc. A* **2017**, *375*, 20170014.
[21] H. Böhrer, N. Trapp, D. Himmel, M. Schleep, I. Krossing, *Dalton Trans.* **2015**, *44*, 7489–7499.
[22] A. Y. Timoshkin, G. Frenking, *Organometallics* **2008**, *27*, 371–380.
[23] a) V. I. Trusov, A. V. Suvorov, *Zh. Neorg. Khim.* **1974**, *19*, 3253–3256; b) V. I. Trusov, A. V. Suvorov, A. S. Tarasova, *Zh. Neorg. Khim.* **1976**, *21*, 3102–3106.
[24] A. Y. Timoshkin, H. F. Bettinger, H. F. Schaefer, *J. Am. Chem. Soc.* **1997**, *119*, 5668–5678.
[25] N. A. Shcherbina, I. V. Kazakov, N. Yu. Gugin, A. S. Lisovenko, A. V. Pomogaeva, Yu. V. Kondrat'ev, V. V. Suslonov, A. Y. Timoshkin, *Russ. J. Gen. Chem.* **2019**, *89*, 1162–1168.
[26] a) H. Jacobsen, H. Berke, S. Döring, G. Kehr, G. Erker, R. Fröhlich, O. Meyer, *Organometallics* **1999**, *18*, 1724–1735; b) C. Bergquist, B. M. Bridgewater, C. J. Harlan, J. R. Norton, R. A. Friesner, G. Parkin, *J. Am. Chem. Soc.* **2000**, *122*, 10581–10590.
[27] Z.-H. Choi, W. Tyrra, A. Adam, *Z. Anorg. Allg. Chem.* **1999**, *625*, 1287–1292.
[28] J. Emsley, *The Elements*, 3rd ed., Clarendon Press, **1998**, pp 300.
[29] See Supporting Information for details.
[30] a) T. N. Sevastianova, A. V. Suvorov, *Russ. J. Coord. Chem.* **1999**, *25*, 679–688; b) E. I. Davydova, T. N. Sevastianova, A. V. Suvorov, A. Y. Timoshkin, *Coord. Chem. Rev.* **2010**, *254*, 2031–2077; c) I. V. Kazakov, M. Bodensteiner, A. S. Lisovenko, A. V. Suvorov, M. Scheer, G. Balazs, A. Y. Timoshkin, *Inorg. Chem.* **2013**, *52*, 13207–13215; d) T. N. Sevastianova, E. I. Davydova, I. V. Kazakov, A. Y. Timoshkin, *Russ. Chem. Bull.* **2015**, *64*, 2523–2535.
[31] a) N. P. Wells, J. A. Phillips, *J. Phys. Chem. A* **2002**, *106*, 1518–1523; b) A. A. Eigner, J. A. Rohde, C. C. Knutson, J. A. Phillips, *J. Phys. Chem. B* **2007**, *111*, 1402–1407.
[32] Yu. V. Kondrat'ev, A. V. Butlak, I. V. Kazakov, A. Y. Timoshkin, *Therm. Acta* **2015**, *622*, 64–71.
[33] S. A. Shchukarev, *Russ. Zh. Fiz.-Khem. Soc.* **1924**, *55*, 467 (in Russian).
[34] D. V. Korol'kov, *Periodicity principle in chemistry of main group elements*, SPbU publishing, SPb, **1992**, p. 103 (in Russian).
[35] K. Frąckiewicz, M. Czerwiński, S. Siekierski, *Eur. J. Inorg. Chem.* **2005**, *19*, 3850–3856.
[36] G. Brauer, *Handbook of Preparative Inorganic Chemistry*, second edition Academic press, New York, **1963**, p. 843–845.
[37] G. M. Sheldrick, *Acta Crystallogr., Sect. A* **2008**, *64*, 112–122.
[38] O. V. Dolomanov, L. J. Bourhis, R. J. Gildea, J. A. K. Howard, H. Puschmann, *J. Appl. Crystallogr.* **2009**, *42*, 339–341.
[39] CrysAlisPro, Agilent Technologies, Version 1.171.36.20 (release 27–06–2012).
[40] D. A. Doinikov, I. V. Kazakov, I. S. Krasnova, A. Y. Timoshkin, *Russ. J. Phys. Chem.* **2017**, *91*, 1603–1608.
[41] E. I. Davydova, D. A. Doinikov, I. V. Kazakov, I. S. Krasnova, T. N. Sevast'yanova, A. V. Suvorov, A. Y. Timoshkin, *Russ. J. Gen. Chem.* **2019**, *89*, 1069–1084.
[42] M. J. Frisch, G. W. Trucks, H. B. Schlegel, G. E. Scuseria, M. A. Robb, J. R. Cheeseman, G. Scalmani, V. Barone, G. A. Petersson, H. Nakatsuji, X. Li, M. Caricato, A. V. Marenich, J. Bloino, B. G. Janesko, R. Gomperts, B. Mennucci, H. P. Hratchian, J. V. Ortiz, A. F. Izmaylov, J. L. Sonnenberg, D. Williams-Young, F. Ding, F. Lipparini, F. Egidi, J. Goings, B. Peng, A. Petrone, T. Henderson, D. Ranasinghe, V. G. Zakrzewski, J. Gao, N. Rega, G. Zheng, W. Liang, M. Hada, M. Ehara, K. Toyota, R. Fukuda, J. Hasegawa, M. Ishida, T. Nakajima, Y. Honda, O. Kitao, H. Nakai, T. Vreven, K. Throssell, J. A. Montgomery Jr., J. E. Peralta, F. Ogliaro, M. J. Bearpark, J. J. Heyd, E. N. Brothers, K. N. Kudin, V. N. Staroverov, T. A. Keith, R. Kobayashi, J. Normand, K. Raghavachari, A. P. Rendell, J. C. Burant, S. S. Iyengar, J. Tomasi, M. Cossi, J. M. Millam, M. Klene, C. Adamo, R. Cammi, J. W. Ochterski, R. L. Martin, K. Morokuma, O. Farkas, J. B. Foresman, D. J. Fox, Gaussian 16, Revision A.03; Gaussian, Inc.: Wallingford, CT, 2016.
[43] A. D. Becke, *J. Chem. Phys.* **1993**, *98*, 1372–1377.
[44] C. Lee, W. Yang, R. G. Parr, *Phys. Rev. B* **1988**, *37*, 785–789.
[45] F. Weigend, R. Ahlrichs, *Phys. Chem. Chem. Phys.* **2005**, *7*, 3297–3305.
[46] Y. Zhao, D. G. Truhlar, *Theor. Chem. Acc.* **2008**, *120*, 215–241.
[47] a) S. F. Boys, F. Bernardi, *Mol. Phys.* **1970**, *19*, 553–566; b) S. Simon, M. Duran, J. J. Dannenberg, *J. Chem. Phys.* **1996**, *105*, 11024–11031.

[48] F. B. van Duijneveldt, J. G. C. M. van Duijneveldt-van de Rijdt, J. H. van Lenthe, *Chem. Rev.* **1994**, *94*, 1873–1885.
[49] A. V. Marenich, C. J. Cramer, D. G. Truhlar, *J. Phys. Chem. B* **2009**, *113*, 6378–6396.
[50] E. D. Glendening, A. E. Reed, J. E. Carpenter, F. Weinhold, NBO Version 3.1, Gaussian Inc., Pittsburgh, **2003**.

Received: January 27, 2020
Published Online: ■

Journal of Inorganic and General Chemistry
ZAAC
Zeitschrift für anorganische und allgemeine Chemie

ARTICLE